

Anchorage and residual bond characteristics of 7-wire strand
Orr et al

Highlights

- 31 specimens with 7-wire strand are subject to pull out tests;
- The effects of inadequate cover and reinforcement detailing are investigated;
- Specimens with negative cover can retain significant pull out capacity;
- Confinement from transverse reinforcement and cover must be considered together;
- A capacity assessment method is proposed.

1 **Abstract**

2 The periodic assessment of our existing concrete infrastructure is a crucial part of
3 maintaining appropriate levels of public safety over long periods of time. It is important
4 that realistic predictions of the capacity of existing structures can be made in order to
5 avoid unnecessary and expensive intervention work. Assessment is currently
6 undertaken using codified models that are generally readily applied to infrastructure
7 with simple geometric and reinforcement details that conform to design methods for
8 new structures.

9 This approach presents two significant challenges for prestressed structures:
10 1) design and construction practice has changed significantly in the past 50 years, and
11 modern codified approaches can be incompatible with historic structures; and
12 2) deterioration of exposed soffits can lead to reduced cover to internal prestressing
13 strand. Unless appropriate reductions are used in assessment of a structure with such
14 problems, unnecessary load restrictions, or major strengthening or reconstruction work
15 may be required, despite having carried a full service load since its construction.

16 There are currently no widely accepted methods for the prediction of peak and
17 residual capacities in prestressed concrete beams with inadequately detailed 7-wire
18 strand. This paper presents a completely new prediction methodology, validated
19 against new experimental results from 31 novel semi-beam tests. The proposed
20 models for peak load, residual load, and bond stress-slip modelling provide reliable,
21 accurate, and conservative results. Their results demonstrate feasible and appropriate
22 capacity reduction factors for use in the assessment of existing concrete infrastructure.

1

Notation

\emptyset	Nominal strand diameter (mm)
d	Effective depth to flexural reinforcement (mm)
c	Cover to strand (mm)
b	Breadth (mm)
L	Length (mm)
δ_1	Modification factor accounting for reduced cover
δ_2	Modification factor accounting for confinement from cover and/or transverse reinforcement
δ_3	Modification factor accounting for confinement from transverse reinforcement
δ_4	Modification factor accounting for confinement from cover
F	Force (N)
σ_{pd}	Strand Stress (MPa)
A_{ps}	Cross sectional area of strand (mm ²)
l_{bpd}	Total anchorage length for anchoring a tendon with stress σ_{pd} (mm)
l_{pt2}	120% of the basic transmission length (mm)
σ_{pd}	Prestress after all losses (MPa)
σ_{pm0}	Tendon stress just after release (MPa)
f_{bpd}	Bond strength of the concrete at the test date (MPa)
f_{bpt}	Bond stress at transfer (MPa)
$f_{ctd(t)}$	Axial tensile strength of the concrete at release (MPa)
f_{ctd}	Axial tensile strength of the concrete (MPa)
$f_{ctm(te)}$	Mean axial tensile strength at the test date (MPa)
$f_{ctm(tr)}$	Mean axial tensile strength measured at transfer
$\tau_{b,max}$	Maximum value of bond stress (MPa)
s	Slip (relative displacement of strand and concrete) (mm)
L_b	Bonded length (mm)
R_m	Strand tensile strength (MPa)

2

3

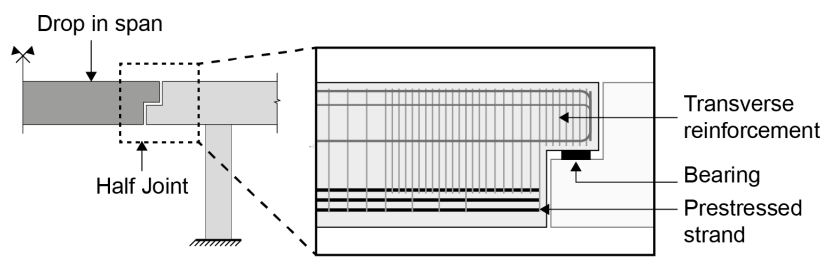
1 Introduction

The periodic assessment of existing infrastructure is crucial to maintain appropriate levels of safety over long periods of time. Changes in loading, material properties, design, detailing, and construction practices mean that some infrastructure, when assessed today, is deemed to be structurally inadequate. Assessment methods that can properly and accurately predict the behaviour of such structures are therefore crucially important to avoid unnecessary and expensive reconstruction works.

Road infrastructure provides a crucial economic pathway, and trunk route road closures have significant economic impacts. Minimising closures to bridges and other infrastructure for repair can therefore provide economic benefits. In the USA, 67,000 (11%) of bridges have been deemed as structurally deficient with load restrictions or closures, and the ASCE estimates \$76 billion is required for their repair or replacement [1]. In the UK road infrastructure investment of £15 billion is already planned for the period to 2021 [2]. Such levels of repair and refurbishment are significant, and must be supported by the provision of appropriate assessment methodologies.

1.1 Half joint bridges

Half joints (Figure 1) have historically been used to simplify the design and construction of bridges. However, due to inspection, construction, and maintenance problems with such designs BD 57 [3] cl.2.2 now notes that half joints should not be used for new bridges unless there is absolutely no alternative. The structural assessment of structures containing half-joints at the serviceability and ultimate limit states in the UK is undertaken using strut and tie models in accordance with BD 44 [4] and BA 39 [5]. Such approaches are readily applicable to cases with simple geometric and reinforcement detailing and when the reinforcement is appropriately anchored.



28

29 **Figure 1: Half joint bridges**

30 If reinforcement in existing structures does not provide theoretically sufficient
 31 anchorage to be fully utilised in a strut and tie model, reduction factors are applied by
 32 the assessing engineer. Common issues where this may arise include 1) loss of cover
 33 due to environmental deterioration; 2) inadequate cover from design detailing; and 3)
 34 transverse reinforcement that does not enclose longitudinal reinforcement. A modern
 35 assessment of a structure with such problems, which may have carried the full service
 36 load since its construction, could lead to load restrictions, strengthening or
 37 reconstruction work, if realistic and appropriate assessment methods, including
 38 consideration of reliability and reduction factors, are not known and used.

39 Some half joint bridges assessed using BD 44 [4] and BA 39 [5] have recently been
 40 rated as provisionally substandard. Although such bridges are now being traffic
 41 managed using BD 79 [6], they had previously been carrying unrestricted traffic loading
 42 since their construction in the 1970s.

43 This paper investigates the effect of loss of cover on bond, peak load, and residual
 44 behaviour for specimens with 7-wire strand as flexural reinforcement. A series of semi-
 45 beam pull out tests were undertaken utilising both unstressed and pretensioned strand
 46 to develop new guidance on appropriate reduction factors for the assessment of half-
 47 joint bridges and, in general, prestressed concrete elements containing theoretically
 48 inadequate 7-wire strand detailing.

49 **2 Bond and anchorage**

50 **2.1 Bond tests**

51 Tests are required to determine the bond characteristics of concrete reinforcement in
52 order to effectively predict required transmission (transfer) and anchorage
53 (development) lengths. Simple cube pull out tests are commonly used (see for example
54 RILEM [7] and ASTM [8] methods) and considerable data for these exists [9-12]. Such
55 tests, however, provide very localised data over small bonded lengths. BS 4449 [13]
56 overcomes this limitation through the use of a half-beam test setup, similar to the
57 'beam end test' of ASTM A944 [14].

58 A simplification of the half-beam test method was proposed by Perera *et al* [15] in
59 which one half of the specimen is tested, whilst retaining the correct state of stress in
60 the end zone. This approach has numerous advantages, including a simpler test set
61 up, and the ability to keep the bar straight rather than deforming it under loading. This
62 method was adopted in this paper for testing unstressed specimens (Figure 4).

63 **2.2 Strand bond**

64 **2.2.1 Unstressed strand**

65 The majority of previous studies of bond of prestressing strand, has been on
66 unstressed samples. Unstressed 7-wire strand achieves bond with the surrounding
67 concrete through adhesion and mechanical interlock. Once slip occurs, adhesion is no
68 longer present and bond will therefore rely only on the mechanical interlock provided
69 by the helical shape of the strand. Unlike for plain and deformed passive reinforcement
70 [16], there is no well-established bond stress-slip model for prestressing strand, yet
71 such a model is crucial for the realistic assessment of existing structures.

72 To determine the bond-slip performance of steel wire strand, Moustafa [17]
73 developed a pull out test in which multiple strands are pulled from a large concrete
74 block, while the Post-Tensioning Institute (PTI) Bond Test uses a single strand pulled
75 from a cement mortar cylinder. The North American Strand Producers (NASP) Bond
76 Test was derived from the PTI method and subsequently adopted by the USA
77 Transport Research Board [18]. The strand is pulled from the cylinder at 24 hours, with
78 the free-end slip of the strand measured. A revised version of the NASP bond test is
79 the Standard Test for Strand Bond (STSB), adopted by the ASTM [19]. Pull out forces
80 and slips are measured for the strand cast into a mortar cylinder. The NASP test
81 provides only a proxy result since the strand is tested in a cylinder of mortar, with the
82 pull out value then being correlated to codified requirements for transmission lengths
83 for strand in concrete.

84 Logan [20] performed 216 pull out tests on 13mm diameter strands from six different
85 manufacturers using the method proposed by Moustafa [17], and showed considerable
86 variation in performance between manufacturers. When compared to flexural beam
87 tests it was however found that the pull out was a useful proxy for comparing
88 behaviour. The variation between manufacturers is also reported by Ramirez and
89 Russell [18] during round robin testing using the NASP test. This suggests that
90 characterising as far as possible properties of the actual strand used in any beam to be
91 assessed is important.

92 Rose and Russell [21] reported an increase in bond strength for strand with a uniform
93 surface coating of rust (achieved over a period of three days exposure in high humidity,
94 wet spray environment) prior to casting. Their work assessed the effects of strand with
95 minor corrosion being used in new construction, and as such may not be not
96 representative of the effect of rusting a steel strand in-situ (which implies that the
97 environmental conditions within the concrete have changed, for example through loss

98 of alkalinity of the concrete or loss of concrete cover), which would seriously
99 compromise the strand to concrete bond.

100 **2.2.2 Stressed strand**

101 In addition to adhesion and mechanical bond, stressed strand obtains further
102 anchorage from the 'Hoyer effect' [22]. The Hoyer effect occurs after the stress in the
103 strand is released into the concrete. Elastic expansion, dilation, and helical strain in the
104 strand result in radial forces in the concrete. These radial forces enhance friction and
105 provide a wedge effect.

106 The length over which prestress force is transferred into the concrete section may be
107 determined by measuring slip at the end of a concrete member and strain on the
108 concrete face parallel to the strand after release of the prestress, while anchorage
109 lengths are typically assessed using pull out tests on unstressed strands as described
110 above.

111 The challenge of achieving a robust test method for prestressed strand is discussed by
112 Marti-Vargas *et al* [23]. Building on work by Cousins *et al* [24], Marti-Vargas *et al* [23]
113 proposed a test method that uses a concentrically positioned pretensioned bar pulled
114 out of a concrete prism, referred to as the 'ECADA' test. Testing a range of prism
115 lengths allows the anchorage and transmission lengths to be estimated and provides
116 load-slip responses for different embedment lengths.

117 Higher strength concretes (up to 80MPa) typically allow shorter anchorage lengths [24].
118 Barnes and Burns [25] found an inversely proportional relationship between the
119 concrete strength and transmission length, although significant scatter was also seen
120 in the test data.

2.2.3 Effect of loss of cover on strand bond

BS EN 1992-1-1 [26] specifies that the minimum cover required to maintain bond to 7-wire strand is 1.5ϕ , where ϕ is the strand diameter (greater cover may be required for other reasons). Force transfer between the tendon and the concrete is modelled by Tepfers [27] using radially directed compressive stresses equilibrated by circumferential tensile stresses. The confining effect of the concrete is determined by the maximum tensile stress that can be carried before cracking of the concrete. Splitting failure can occur when cover distances are low [28]. Various models in the literature use this approach to determine the effect of concrete cover on transmission and anchorage lengths [29].

There have been very few tests on specimens with stressed 7-wire strand where cover distance was a test variable. Deatherage and Burdette [30] tested full scale bridge girders with cover of between 2.5ϕ and 3ϕ and found no difference in anchorage lengths for 15mm strand, an unsurprising result given the BS EN 1992-1-1 [26] limit above. Den Uijl [31] tested smaller specimens with cover distances between 1.36ϕ and 3.0ϕ to determine minimum cover requirements to prevent splitting failures. A reduction in transmission length as cover increases was found, proposed to be due to the non-linear response of the concrete to the wedging effect at tendon release.

Despite a large amount of testing of cube and half-beam specimens to determine bond characteristics of specimens with adequate cover distances (well designed specimens) no data was found in the literature for such semi-beam tests where the test bar has low or negative cover distance (i.e the reinforcement is partially exposed), a key focus of this paper.

144 **2.2.4 Effect of corrosion on strand bond**

145 Rogers *et al* [32] performed destructive tests on 19 decommissioned bridge beams
146 dating from 1969, all of which had suffered corroded pre-tensioned reinforcement due
147 to a high-chloride environment. The beams contained both pretensioned and post-
148 tensioned reinforcement, had a design concrete strength of 38MPa, and mild steel
149 transverse reinforcement. Twelve pre-tensioned strands of 12.7mm diameter were
150 used in each beam, and these strands were unenclosed by the transverse
151 reinforcement. Longitudinal cracking in the soffit of the beams was noted during
152 inspections, subsequently found to be a result of chloride induced corrosion
153 propagating from the corner strand into the specimen until delamination of the cover
154 zone occurred.

155 The 19 beams were tested in three point bending. A combination of shear and
156 flexural failures was recorded. The corroded beams showed between 10% and 32%
157 loss in capacity when compared to beams in a 'good' condition. The magnitude of the
158 capacity reduction was approximately in line with the loss of pre-tensioned strand due
159 to corrosion. The authors' results suggest that the use of non-destructive methods to
160 determine corrosion in strand can be used as an indicator of the actual capacity of a
161 beam under assessment.

162 **2.3 Summary**

163 A broadly accepted model for the pull out characteristics of prestressing strand is
164 not currently available as it is for plain and deformed bars. It is noted in much of the
165 literature that cover distances are important for determining splitting or pull out failures,
166 especially when the presence of transverse reinforcement can confine concrete around
167 the strand. However no data is available for the pull out testing of beams with strand
168 that has low or negative cover distances. This is important since corroded or spalled

169 structures may have such low (or negative) cover and their residual capacity needs to
170 be able to be quantified.

171 **3 Testing**

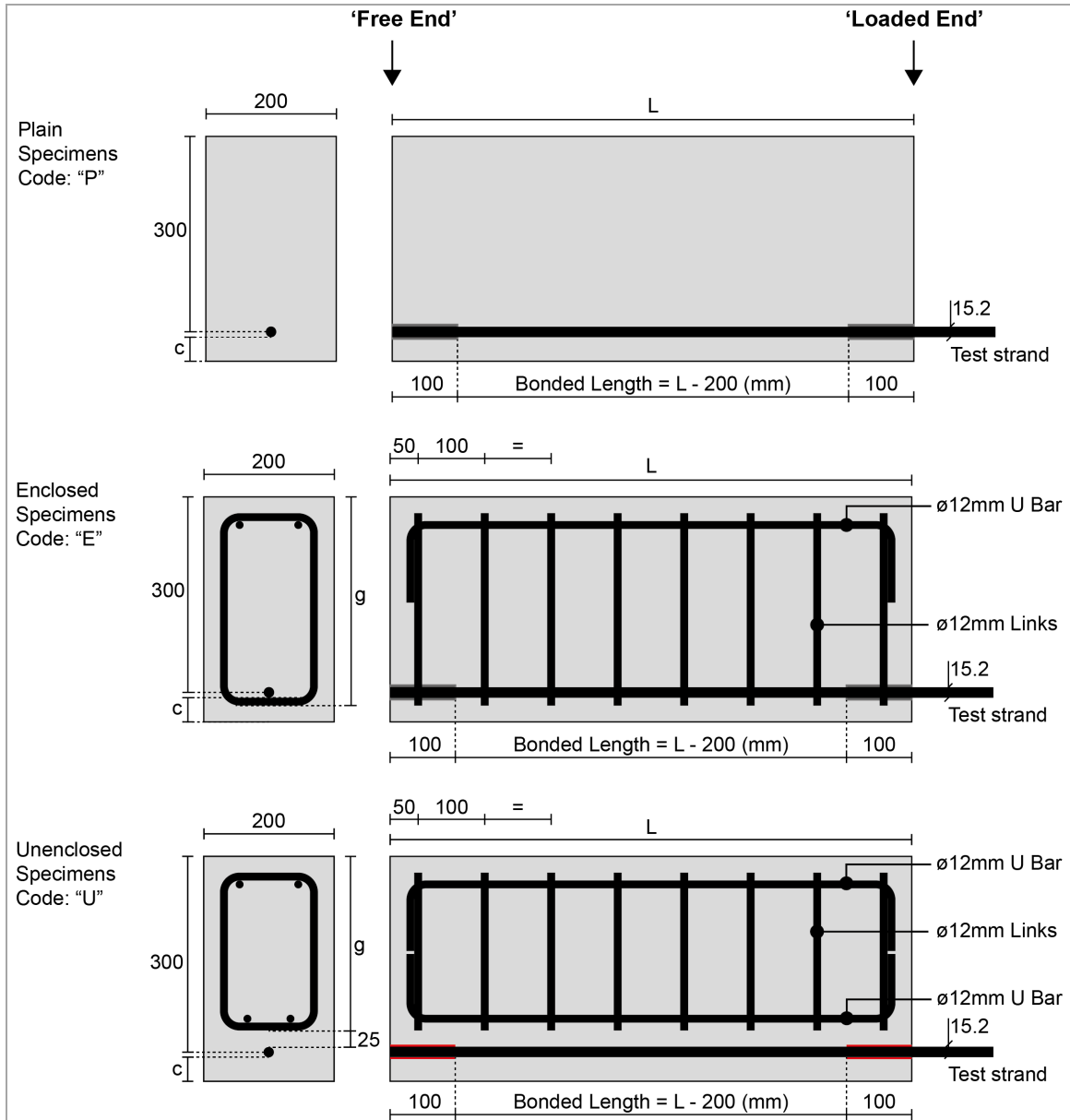
172 To determine the pull out behaviour of 15.2mm diameter 7-wire strand and provide new
173 guidance on appropriate reduction factors for assessment, a series of semi-beam tests
174 were undertaken to determine for the first time the effect of loss of cover on bond, peak
175 load, and residual load in specimens with both unstressed and prestensioned strand.

176 **3.1 Test design**

177 A total of 31 semi-beam specimens were tested, 19 with unstressed strand and 12 with
178 stressed strand. Both stressed and unstressed specimens were tested in order to
179 identify any specific pull out behaviour arising from prestressing of the strand. All
180 specimens were designed with an effective depth to the strand of 300mm and breadth
181 of 200mm. All strand was 15.2mm in diameter (\emptyset). The test variables were: bonded
182 length (300mm ($\approx 20\emptyset$), 600mm ($\approx 40\emptyset$), or 900mm ($\approx 60\emptyset$)), cover distance to the strand
183 (37mm, 0mm, or -8mm), and transverse reinforcement design (Plain ('P'), Enclosed
184 ('E'), or Unenclosed ('U'), as shown in Figure 2). The specimens are summarised in
185 Table 1.

186 Specimens with negative cover (-8mm) have half the diameter of the strand outside
187 of the concrete section. For specimens with -8mm cover *and* enclosed transverse
188 reinforcement ('E'), the transverse reinforcement necessarily also sits outside the
189 concrete section. See also Figure 14.

190 The prismatic test specimens have a support condition beneath the strand, whereas
191 this is more remote in a real half-beam joint. The pragmatic test set up was chosen to
192 reflect reality as far as possible, but it is important to realise this potential limitation.



193

194 **Figure 2: Specimen dimensions**

195 **Table 1: Test specimen details**

Specimen Code ^a	Initial prestress (% R_m)	Transverse reinforcement type ^b	Dimension g (mm) ^c	Length, L (mm) ^d	Bonded length (mm) ^e	Cover, c (mm) ^f
0/P/300/37	0	P	0	500	300	37
0/P/300/0	0	P	0	500	300	0
0/P/600/37	0	P	0	800	600	37
0/P/600/0	0	P	0	800	600	0
0/E/300/37	0	E	320	500	300	37
0/E/300/0	0	E	320	500	300	0
0/E/300/-8	0	E	320	500	300	-8
0/E/600/37	0	E	320	800	600	37

Specimen Code ^a	Initial prestress (% R _m)	Transverse reinforcement type ^b	Dimension g (mm) ^c	Length, L (mm) ^d	Bonded length (mm) ^e	Cover, c (mm) ^f
0/E/600/0	0	E	320	800	600	0
0/E/600/-8	0	E	320	800	600	-8
0/E/900/37	0	E	320	1100	900	37
0/E/900/0	0	E	320	1100	900	0
0/E/900/-8	0	E	320	1100	900	-8
0/U/600/37	0	U	267	800	600	37
0/U/600/0	0	U	267	800	600	0
0/U/600/-8	0	U	267	800	600	-8
0/U/900/37	0	U	267	1100	900	37
0/U/900/0	0	U	267	1100	900	0
0/U/900/-8	0	U	267	1100	900	-8
55/E/600/37	55	E	320	800	600	37
55/E/600/0	55	E	320	800	600	0
55/E/600/-8	55	E	320	800	600	-8
69/E/900/37	69	E	320	1100	900	37
69/E/900/0	69	E	320	1100	900	0
69/E/900/-8	69	E	320	1100	900	-8
55/U/600/37	55	U	267	800	600	37
55/U/600/0	55	U	267	800	600	0
55/U/600/-8	55	U	267	800	600	-8
69/U/900/37	69	U	267	1100	900	37
69/U/900/0	69	U	267	1100	900	0
69/U/900/-8	69	U	267	1100	900	-8

Notes: ^a Specimen Code: Initial Prestress % [0 (unstressed), 55%, or 69%] / Transverse Reinforcement Type [P, E, U, Figure 5] / Bonded Length [300, 600, or 900mm] / Cover [37, 0, or -8mm], ^{b,c,d,e,f} See Figure 5.

196 **3.1.1 Design parameters**

197 An average concrete cube compressive design strength of 50MPa for all specimens
198 was chosen, to replicate typical concrete strengths found in historic examples of
199 prestressed concrete beams provided by Highways England. A concrete mix was
200 designed to achieve a compressive strength of 50MPa at the test date (14 days after
201 casting) and is given in Table 2. Six 100mm cubes and 100mm cylinders were cast
202 alongside each test specimen in accordance with BS EN 12390-2 [33] for compressive
203 strength testing [34] and tensile splitting testing [35]. All specimens were demoulded 24
204 hours after casting.

205 Bridon 7-wire 15.2mm diameter 1670 Grade strand was used in all specimens,
 206 Table 3. A tension test was undertaken on a sample of the 15.2mm diameter strand, as
 207 shown in Figure 3, where stresses are calculated using a cross sectional area of
 208 139mm² (Table 3).

209 Bonded lengths of 300, 600, and 900mm were chosen based on prediction
 210 calculations following BS EN 1992-1-1 [26] such that all specimens would fail in pull out
 211 (rather than strand yield) whilst also giving a range of bonded areas to consider in the
 212 analysis.

213 Where present, all other reinforcement in the test specimens was 12mm diameter
 214 deformed bar grade B500C [36]. Cover to the transverse reinforcement was 25mm.
 215 None of the specimens with transverse reinforcement failed in shear.

216 **Table 2: Mix design per m³**

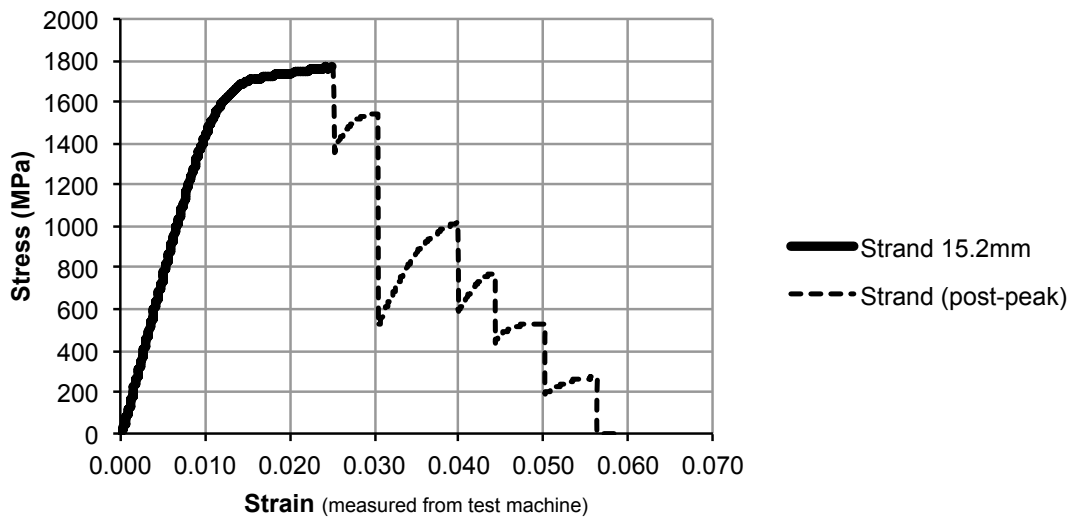
CEM I 42.5N Cement (kg)	Tap water (kg)	Coarse aggregate (12-14mm)	Fine aggregate (<5mm)
620	210	865	710

217

218 **Table 3: 1670 Grade Strand, manufacturer's data [37] following prEN 10138 [38]**

Type	Nominal diameter (mm)	Nominal values only				Specified characteristic values		Typical values
		Tensile strength (R _m) N/mm ²	Steel area (mm ²)	Mass (kg/m)	Mass (m/1000kg)	Breaking load (F _m) kN	0.1% Proof load (F _{p0.1}) kN	Load at 1% elongation (F _{t 1.0}) kN
Standard	15.2	1670	139.0	1.090	917	232.0	204.0	204

219



220

221 **Figure 3: Load-displacement results for 15.2mm strand as tested**

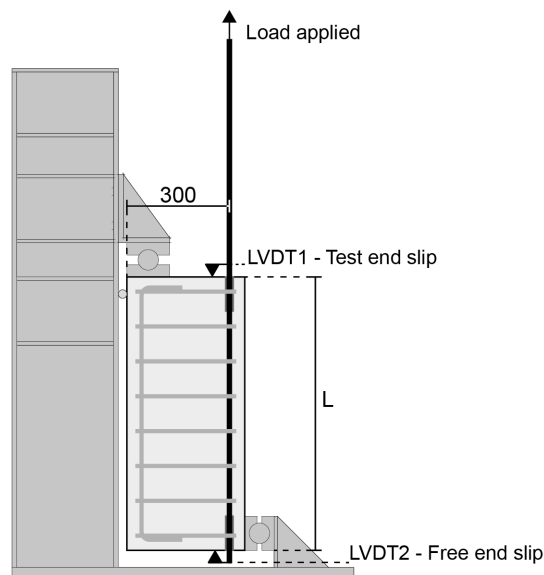
222 **3.1.2 Stressed strand specimens**

223 Twelve specimens were tested with pre-tensioned strand. The specimens had bonded
 224 lengths of 600mm or 900mm (Table 1). Strand stresses were chosen based on
 225 information provided by Highways England for historic stressed strand specimens.
 226 Specimens with 600mm bonded length were pretensioned to an initial stress of
 227 916MPa ($0.55R_m$) and specimens with 900mm bonded length were pretensioned to
 228 1145MPa ($0.69R_m$).

229 **3.2 Test method**

230 **3.2.1 Unstressed specimens**

231 All specimens were tested 14 days after casting in the frame shown in Figure 4. Load
 232 was applied to each strand by a 2000kN test machine under stroke control at
 233 2mm/min. Slip of the strand was measured using linear variable displacement
 234 transducers at both the test end and the free end of the specimen (LVDT1 and
 235 LVDT2).



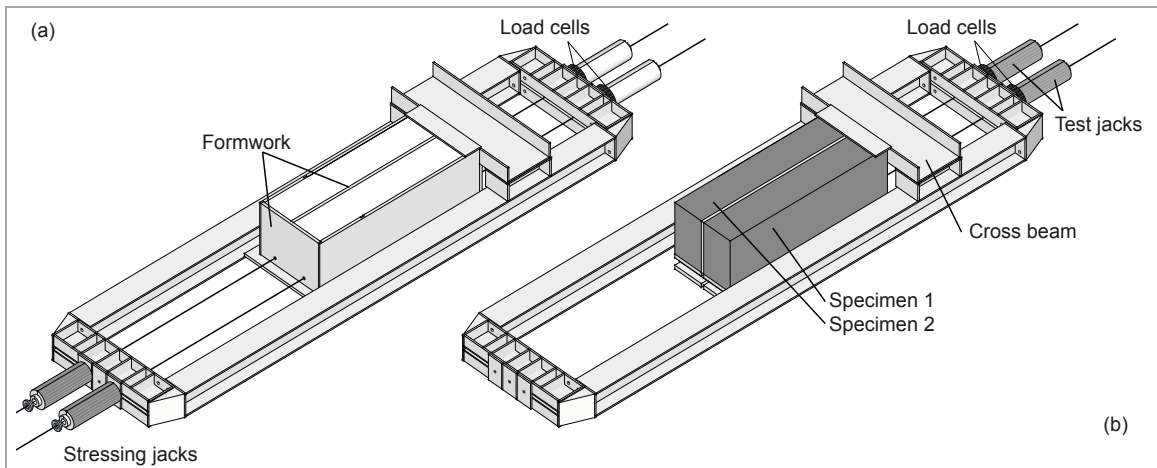
236

237 **Figure 4: Unstressed specimen test method**

238 **3.2.2 Stressed specimens**

239 In a prestressed beam a transmission length is required at both ends of the strand.
 240 When calculated using BS EN 1992-1-1 [26] the transmission length is linearly related
 241 to the tendon stress after release. Therefore a high tendon stress requires a longer
 242 transmission length. To achieve the semi-beam test method with prestressed strand, it
 243 was necessary to maintain the strand tension at the test end of the specimen (Figure 2)
 244 throughout the casting and curing process. This was achieved by stressing, casting
 245 and testing these specimens in pairs in a bespoke frame (see Figure 5).

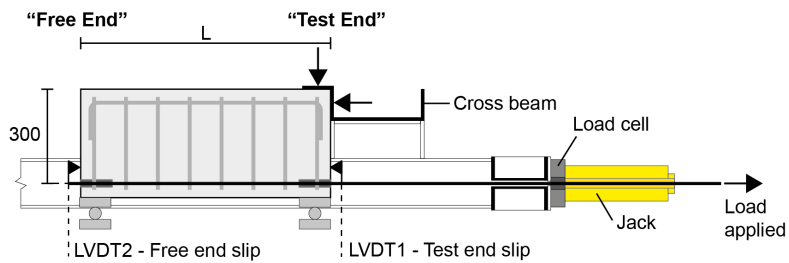
246 Hydraulic jacks were used to apply and maintain the pretension during casting and
 247 curing. After three days the strand stress was released at the free end but was
 248 maintained at the test end by allowing the specimen to react against the test frame
 249 cross beam (Figure 5). After curing, the jacks at the test end of the frame were used to
 250 apply the test load to the stressed strand (Figure 6). One load cell per strand was used
 251 to monitor the strand force throughout the prestressing, curing, and testing phases.



252

253

Figure 5: Stressing and casting arrangement (a); Test arrangement (b)



254

255

Figure 6: Test method, stressed specimens

256

3.3 Results

257

3.3.1 Concrete strength

258

The average concrete compressive cube strength at the test date was 54.2MPa (with a

259

standard deviation of, $\sigma = 4.8\text{MPa}$ from 81 tests). The average concrete split cylinder

260

tensile strength of all specimens at their test date was 3.52MPa ($\sigma = 0.68\text{MPa}$ from 48

261

cylinders). For specimens with stressed strand, the average split cylinder tensile

262

strength at strand detensioning (3 days after casting) was 3.41MPa ($\sigma = 0.68\text{MPa}$ from

263

11 cylinders).

264

3.3.2 Prestress losses

265

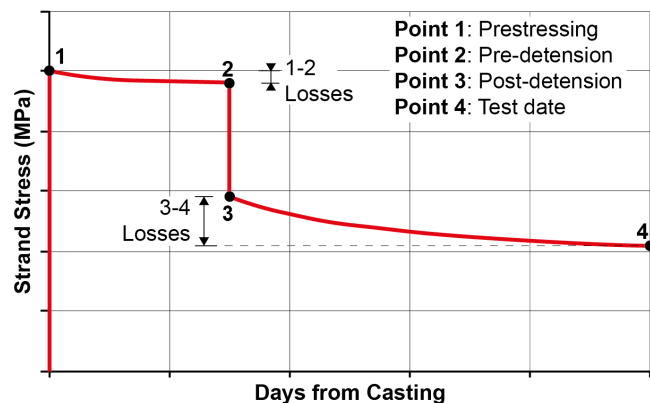
For the prestressed specimens, load cells were used to monitor the strand stress

266

throughout their casting, curing and strand detensioning. The load-time results all

267 followed the same pattern, as summarised in Figure 7. Results for each specimen are
 268 given in Table 4. The strand stress prior to testing after all losses ($\sigma_{pm\infty}$) is given by
 269 Point 4.

270 It is apparent in Table 4 that losses in Specimens 69/U/900/0 and 69/U/900/-8 are
 271 so large as to imply that slip in the prestress zone was sufficient to break the bond
 272 between the strand and the concrete. As shown in Figure 5, the specimens were cast
 273 in pairs. Premature detensioning occurred in the specimen cast alongside 69/E/900/-8,
 274 which caused a small increase in the Point 2 value of prestress recorded for 69/E/900/-
 275 8 (see Table 4). The increase was small enough to not be a concern. The specimen
 276 that suffered premature detensioning was not tested.



277

278 **Figure 7: Typical prestress loss over time indicating Points 1 – 4 in Figure 7**

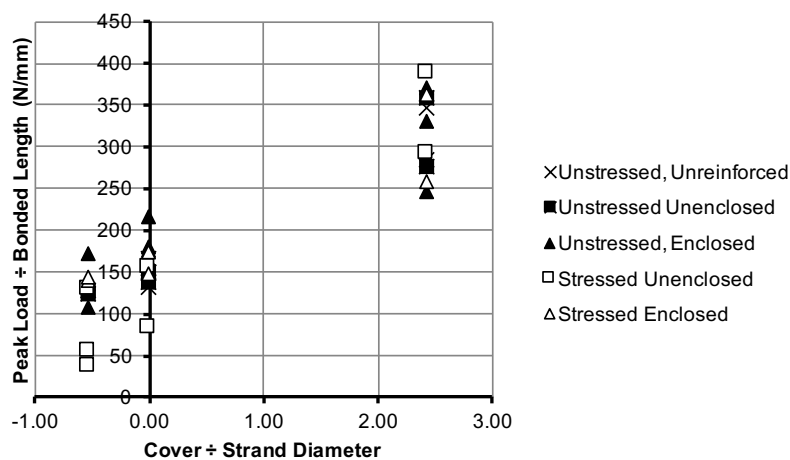
279 **Table 4: Summary of prestress losses**

Code ¹	Cover	Target Prestress	Point 1	Point 2	1-2 Loss (%)	Point 3	Point 4	3 - 4 Loss (%)	Total losses (1-4) (%)
55/E/600/37	37	916MPa	1016MPa	962MPa	5%	626MPa	551MPa	12%	46%
55/E/600/0	0	916MPa	1009MPa	966MPa	4%	575MPa	419MPa	27%	58%
55/E/600/-8	-8	916MPa	993MPa	996MPa	0%	529MPa	428MPa	19%	57%
69/E/900/37	37	1145MPa	1262MPa	1204MPa	5%	955MPa	926MPa	3%	27%
69/E/900/0	0	1145MPa	1261MPa	1233MPa	2%	870MPa	642MPa	26%	49%
69/E/900/-8	-8	1145MPa	1260MPa	1317MPa	-5%	923MPa	693MPa	25%	45%
55/U/600/37	37	916MPa	1004MPa	990MPa	1%	902MPa	871MPa	3%	13%
55/U/600/0	0	916MPa	1000MPa	989MPa	1%	709MPa	464MPa	35%	54%
55/U/600/-8	-8	916MPa	998MPa	1002MPa	0%	631MPa	439MPa	30%	56%
69/U/900/37	37	1145MPa	1256MPa	1241MPa	1%	1144MPa	1091MPa	5%	13%

69/U/900/0	0	1145MPa	1258MPa	1251MPa	1%	478MPa	296MPa	38%	76%
69/U/900/-8	-8	1145MPa	1296MPa	1271MPa	2%	267MPa	172MPa	36%	87%

280 **3.3.3 Peak load**

281 A summary of the peak load achieved in all tests is given in Figure 8, showing peak
 282 load divided by bonded length (N/mm) against cover divided by strand diameter. A
 283 reliable trend is seen in all cases. Further details are given in Table 5 and Table 6
 284 below.



285

286 **Figure 8: Summary of all peak load results**

287 **3.3.3.1 Unstressed specimens**

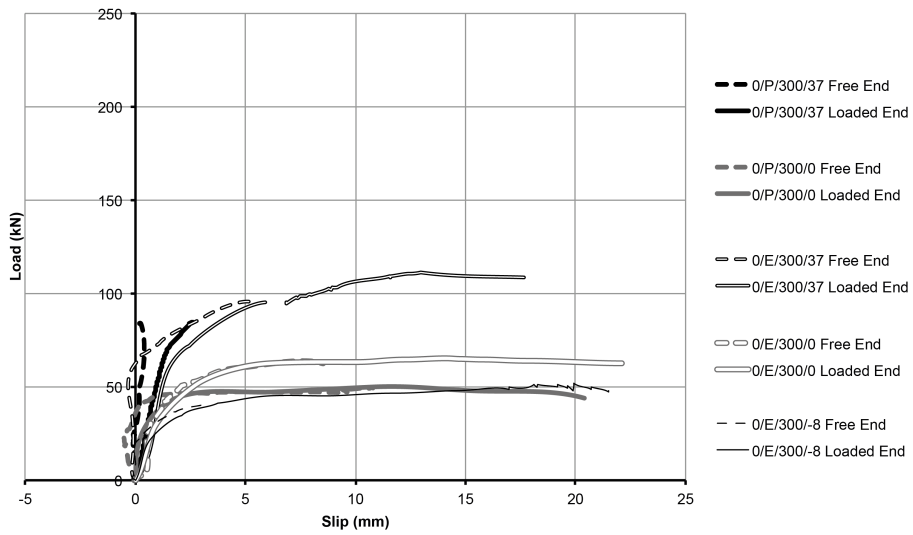
288 The peak and residual loads for each unstressed test are summarised in Table 5. The
 289 applied load versus free end slip is shown in Figure 9 to Figure 11. When represented
 290 on the x-axis of a graph the slip of the strand is defined as the movement of the strand
 291 relative to the specimen concrete face. This is measured with an LVDT secured to the
 292 strand with the probe touching the concrete face. Slip at both the *free end* and the *test*
 293 *end* was recorded for the tests (Figure 4).

294 **Table 5: Summary of unstressed specimen test results**

Code ¹	Peak Load (kN)	Failure Mode	Residual strength (kN)
0/P/300/37	85	Shear	0
0/P/300/0	50	Pull out	47
0/P/600/37	208	Pull out, Shear	0

Code ¹	Peak Load (kN)	Failure Mode	Residual strength (kN)
0/P/600/0	79	Pull out	70
0/E/300/37	111	Pull out	108
0/E/300/0	65	Pull out	62
0/E/300/-8	52	Pull out	46
0/E/600/37	199	Pull out	0
0/E/600/0	108	Pull out	100
0/E/600/-8	65	Pull out	57
0/E/900/37	223	Pull out	-
0/E/900/0	159	Pull out	158
0/E/900/-8	124	Pull out	120
0/U/600/37	216	Pull out	-
0/U/600/0	83	Pull out	73
0/U/600/-8	77	Pull out	70
0/U/900/37	250	Pull out, block failure	168
0/U/900/0	136	Pull out	130
0/U/900/-8	112	Pull out	74

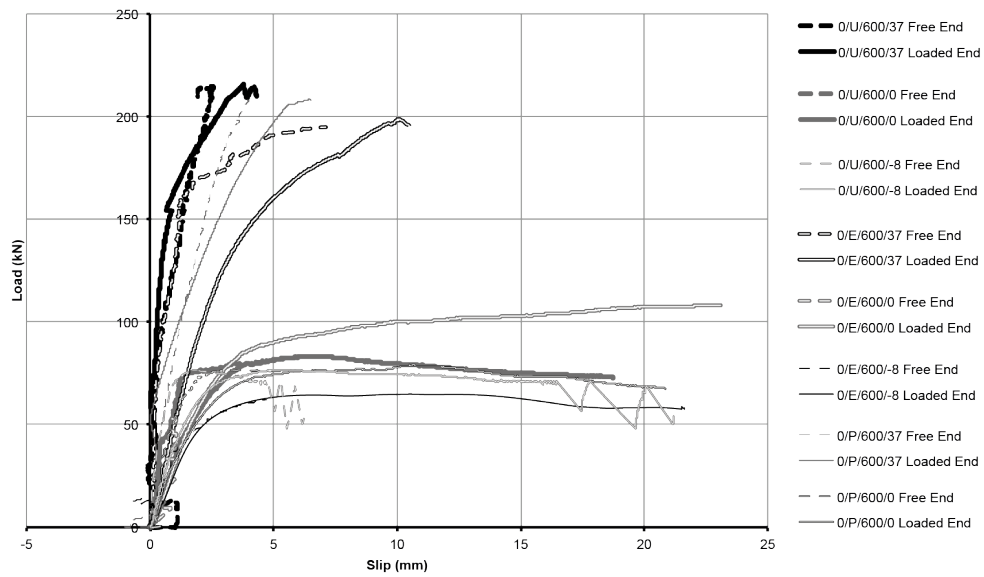
Notes: ¹ See Figure 2 and Table 1.



295

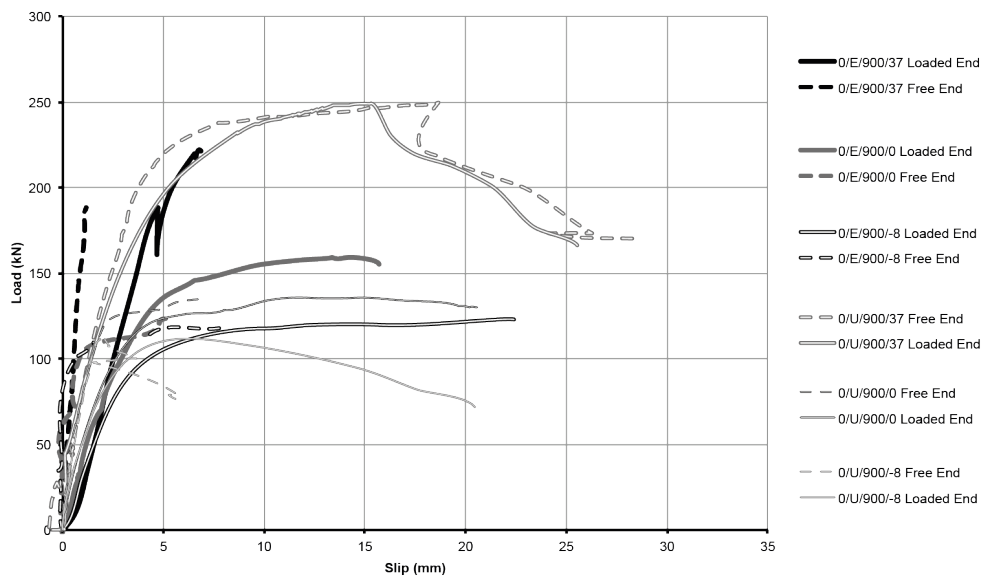
296

Figure 9: Unstressed specimens with 300mm bonded length



297

298 **Figure 10: Unstressed specimens with 600mm bonded length**



299

300 **Figure 11: Unstressed specimens with 900mm bonded length**

301 **3.3.3.2 Load-slip results – stressed specimens**

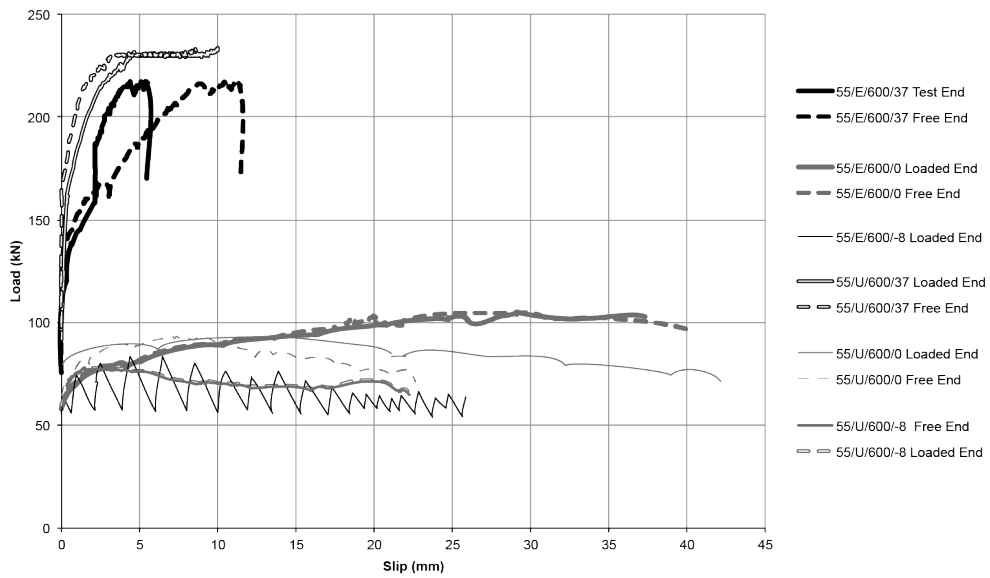
302 The peak and residual loads for each stressed test are summarised in Table 6. The
 303 applied load versus free end slip is shown in Figure 12 - Figure 13.

304

Table 6: Summary of stressed specimen test results

Code ¹	Peak Load (kN)	Failure Mode	Residual strength (kN)
55/E/600/37	217	Pull out	214
55/E/600/0	105	Pull out	100
55/E/600/-8	84	Pull out	64
69/E/900/37	195	Pull out	195
69/E/900/0	131	Pull out	90
69/E/900/-8	129	Pull out	65
55/U/600/37	233	Pull out	233
55/U/600/0	93	Pull out	69
55/U/600/-8	78	Pull out	65
69/U/900/37	264	Strand failure	0
69/U/900/0	77	Pull out	46
69/U/900/-8	34	Pull out	21

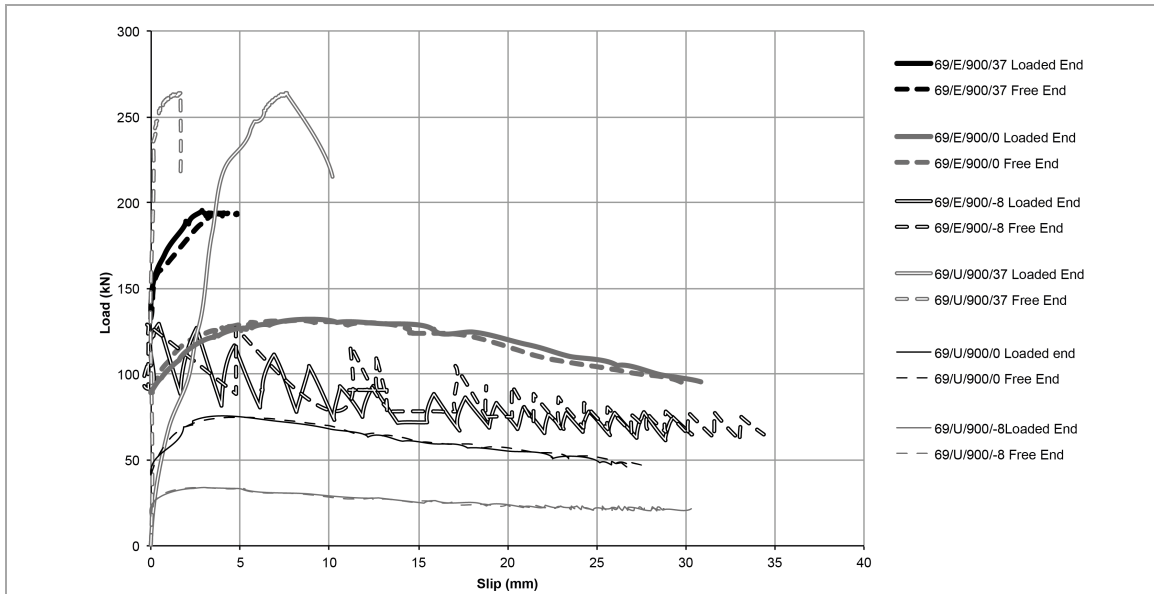
Notes: ¹ See Figure 2 and Table 1.



305

306

Figure 12: Stressed specimens with 600mm bonded length



307

308 **Figure 13: Stressed specimens with 900mm bonded length**

309 Specimens 55/E/600/-8 and 69/E/900/-8 both exhibited the same behaviour during
 310 post-peak pull out. The 'zig-zag' lines shown in Figure 12 (Specimen 55/E/600/-8) and
 311 Figure 13 (Specimen 69/E/900/-8) demonstrate a 'stick-slip' behaviour which was not
 312 seen in any other tests. Both specimens have the same transverse reinforcement, and
 313 -8mm cover, suggesting that the response may be due to the exposed transverse
 314 reinforcement providing additional restraint to the strand during pull out. The maximum
 315 peak-peak amplitude of the stick-slip response is 45kN for 69/E/900/-8 and 27kN for
 316 55/E/600/-8, the ratio of these two amplitudes is 1.67. This is very similar to the ratio of
 317 the number of stirrups crossing the strand in each specimen: nine stirrups enclose
 318 69/E/900/-8 and six stirrups enclose 55/E/600/-8 (ratio of 1.5), suggesting that the
 319 stick-slip behaviour is indeed related to the localised behaviour provided by the stirrups
 320 in these tests.

321 **3.4 Summary**

322 The tests undertaken have demonstrated that specimens with zero or negative cover
 323 can show considerable peak capacity despite their loss of cover. It is seen in the test

324 results that specimens with transverse reinforcement that does not enclose the strand
325 reached similar peak loads to those for which the transverse reinforcement did enclose
326 the strand. Unenclosed specimens provided capacity in excess of what might be
327 expected of a structure in which there is no obvious tension tie between the strand and
328 the compression zone. Specimens with -8mm cover provided significant levels of peak
329 capacity, but post-peak these specimens displayed a descending load-slip curve and
330 provided no plateau at the peak load.

331 **4 Analysis and Modelling**

332 **4.1 Anchorage force**

333 It is proposed that the anchorage capacity of pretensioned beams with inadequate
334 cover can be analysed following the method of BS EN 1992-1-1 [26] Figure 8.17 and
335 applying modification factors that allow the consideration of 1) bonded perimeter (δ_1)
336 and 2) confinement from cover and/or transverse reinforcement (δ_2).

337 It is proposed that the anchorage force capacity (kN) of members with inadequate
338 cover may be predicted using Eq.(1):

$$339 \quad F = (\delta_1)(\delta_2)\sigma_p A_{ps} \quad (1)$$

340 **4.1.1 Modification factor δ_1**

341 Modification factor δ_1 accounts for the reduction in bonded perimeter in specimens with
342 reduced cover, with values given in Eq.(2):

$$343 \quad \begin{array}{ll} c \geq 1.5\phi & \delta_1 = 1.0 \\ 0 \leq c < 1.5\phi & \delta_1 = 0.8 \\ -0.5\phi \leq c < 0 & \delta_1 = 0.5 \\ -0.5\phi < c & \delta_1 = 0.0 \end{array} \quad (2)$$

344 The value of δ_1 is taken as 1.0 when $c \geq 1.5\phi$, based on the minimum cover distance
345 required for full bond of 7-wire strand in BS EN 1992-1-1 [26] (see §2.2.3). As half the
346 bar diameter is exposed for cover distances of -0.5ϕ , a value of $\delta_1 = 0.5$ was chosen,
347 and conservatively applied to the range of $-0.5\phi \leq c < 0$. In the range $0 \leq c \leq 1.5\phi$, the
348 value of δ_1 was calibrated against the peak load test data and chosen as 0.80, ensuring
349 that all predictions presented in Table 7 remain on the conservative side.

350 **4.1.2 Modification factor δ_2**

351 Confinement to strand can be provided by 1) transverse reinforcement, which
352 dominates in specimens with zero or negative cover; and/or 2) concrete cover, which
353 dominates in specimens with larger cover distances.

354 The value for δ_2 is proposed in Eq.(3):

$$355 \quad \delta_2 = \max(\{\delta_3\}, \{\delta_4\}) \geq 1 \quad (3)$$

356 Where δ_3 is the effect of confinement from transverse reinforcement and δ_4 is the
357 effect of confinement from cover. It is assumed that one or other of these dominate the
358 confinement behaviour and that the effects are not additive. It is therefore suggested
359 that the maximum value of the two be taken.

360 *4.1.2.1 Effect of transverse reinforcement (δ_3)*

361 The degree of passive confinement provided by transverse reinforcement is
362 calculated using the approach proposed in the fib Model Code [16], as given in Eq.(4):

$$363 \quad \delta_3 = k_d (K_{tr} - \alpha_t / 50) \geq 0.0, K_{tr} \leq 0.05 \quad (4)$$

$$364 \quad K_{tr} = n_t A_{st} / (n_b \phi s_t) \quad (5)$$

365 Where n_t is the number of legs of confining reinforcement crossing a potential
 366 splitting failure surface at a section; A_{st} is the cross sectional area of one leg of a
 367 confining bar; s_t is the longitudinal spacing of confining reinforcement; n_b is the number
 368 of anchored bars or pairs of lapped bars in the potential splitting failure surface; ϕ is the
 369 diameter of the anchored bar.

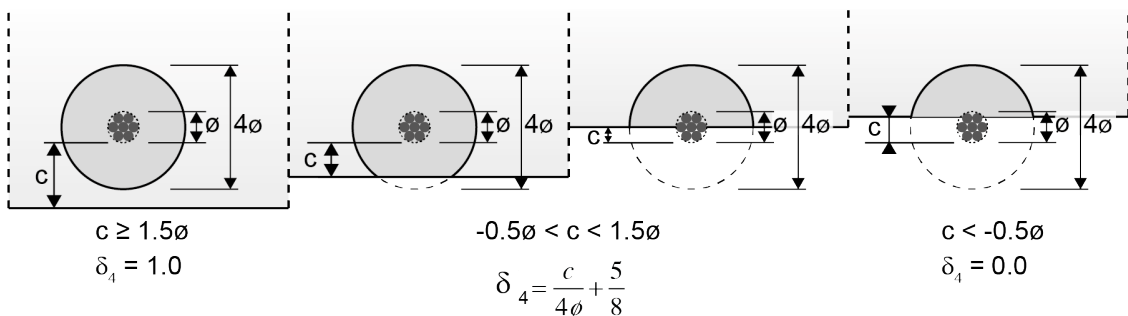
370 For the specimens presented in this paper: $k_d = 20$; $K_{tr} = 0.05$; $\alpha_t = 0.5$.

371 **4.1.2.2 Effect of cover (δ_4)**

372 In order to transmit bond forces, BS EN 1992-1-1 [26] requires members to have a
 373 cover to strand of at least 1.5ϕ . The confining effect of cover on strand is incorporated
 374 as shown in Figure 14, where a cover distance of 1.5ϕ provides full confinement by the
 375 cover, with a linear reduction between 1.5ϕ and -0.5ϕ . At cover distances less than -
 376 0.5ϕ , the concrete provides zero confinement to the strand.

377 The value of δ_4 is given by Eq.(6):

$$\begin{aligned}
 c \geq 1.5\phi & \quad \delta_4 = 1.0 \\
 -0.5\phi \leq c < 1.5\phi & \quad \delta_4 = \frac{c}{4\phi} + \frac{5}{8} \\
 c < -0.5\phi & \quad \delta_4 = 0.0
 \end{aligned}
 \tag{6}$$



379

380 **Figure 14: Definition of modification factor δ_4**

381 **4.1.3 Analysis**

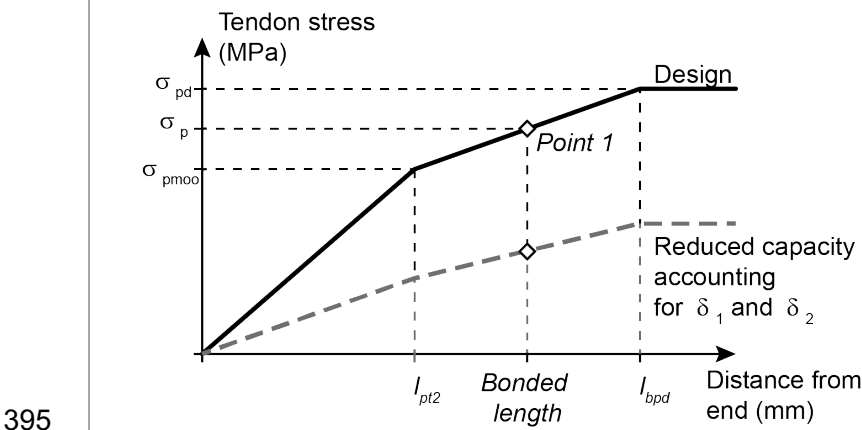
382 The effect of such an approach on BS EN 1992-1-1 [26] Figure 8.17 is illustrated in
 383 Figure 15, where l_{bpd} is the total anchorage length for anchoring a tendon with stress
 384 σ_{pd} as given by Eq.(7), l_{pt2} is 120% of the basic transmission length as given by Eq.(8),
 385 σ_{pd} is the tendon stress, σ_{pmoo} is the prestress after all losses, σ_{pm0} is the tendon stress
 386 just after release; α_1 , α_2 , η_{p1} , η_{p2} , and η_1 are parameters given in BS EN 1992-1-1 [26];
 387 ϕ is the tendon diameter; f_{bpd} is the bond strength of the concrete at the test date as
 388 given by Eq.(9); f_{bpt} is the bond stress at transfer, given by Eq.(10); $f_{ctd(t)}$ is the axial
 389 tensile strength of the concrete at release; f_{ctd} is the axial tensile strength of the
 390 concrete.

391
$$l_{bpd} = l_{pt2} + \alpha_2 \phi (\sigma_{pd} - \sigma_{pmoo}) / f_{bpd} \quad (7)$$

392
$$l_{pt2} = 1.2 (\alpha_1 \alpha_2 \phi \sigma_{pm0} / f_{bpt}) \quad (8)$$

393
$$f_{bpd} = \eta_{p2} \eta_1 f_{ctd} \quad (9)$$

394
$$f_{bpt} = \eta_{p1} \eta_1 f_{ctd(t)} \quad (10)$$



395
 396 **Figure 15: Stresses in the anchorage zone of pre-tensioned members**

397 Once the values shown in Figure 15 are calculated, the tendon stress is predicted
 398 based on the available bonded length (600mm or 900mm in the tests described here).
 399 This point, shown as 'Point 1' in Figure 15, provides a strand stress. Using Eq.(1) the
 400 predicted allowable anchorage force is then determined, multiplying the tendon stress
 401 from Figure 15 (σ_p calculated at available bonded length l) by the cross sectional area
 402 of the tendon and by the modification factors δ_1 and δ_2 .

403 4.1.4 Peak capacity

404 The method described above was undertaken for all stressed specimens and is
 405 summarised in Table 7. Concrete properties are all values measured during testing
 406 from split cylinder tests: f_{ctd} in Eq.(9) is taken as $f_{ctm(te)}$, the mean axial tensile strength
 407 at the test date and $f_{ctd(t)}$ in Eq.(10) is taken as $f_{ctm(tr)}$, the mean axial tensile strength
 408 measured at transfer (concrete axial tensile strengths are obtained by multiplying split
 409 cylinder test results by 0.9).

410 As the prestress was monitored for all specimens from casting through to testing
 411 (Figure 7) the prestress after losses (σ_{pmoo}) is known accurately for all specimens.

412 **Table 7: Peak capacity predictions for all stressed specimens**

Code	δ_1	δ_2	δ_3	δ_4	$f_{ctm(tr)}$ (MPa)	l_{pl2} (mm)	$f_{ctm(te)}$ (MPa)	l_{bpd} (mm)	$\delta_1 \delta_2 (\sigma_{pd})$ (MPa)	$\delta_1 \delta_2 (\sigma_{pmoo})$ (MPa)	σ_p (MPa)	$F_{reduced}$ (kN)	Experimenta l (kN)	Exp/ Pred
55/E/600/37	1.00	1.00	0.80	1.00	2.25	440	3.50	1211	1670	551	783	109	217	1.99
55/E/600/0	0.80	0.80	0.80	0.63	3.59	276	3.38	1167	1069	268	559	78	105	1.35
55/E/600/-8	0.50	0.80	0.80	0.49	2.39	416	2.25	1744	668	171	240	33	84	2.52
69/E/900/37	1.00	1.00	0.80	1.00	2.14	580	2.02	1467	1670	926	1194	166	195	1.17
69/E/900/0	0.80	0.80	0.80	0.63	3.13	397	3.02	1216	1069	411	815	113	131	1.16
69/E/900/-8	0.50	0.80	0.80	0.49	3.64	341	3.67	981	668	277	618	86	129	1.50
55/U/600/37	1.00	1.00	0.00	1.00	3.47	286	2.96	935	1670	871	1257	175	233	1.33
55/U/600/0	0.80	0.63	0.00	0.63	2.30	431	2.61	1543	835	232	324	45	93	2.07
55/U/600/-8	0.50	0.49	0.00	0.49	3.73	266	3.82	1042	412	108	239	33	78	2.35
69/U/900/37	1.00	1.00	0.00	1.00	3.46	358	3.37	772	1670	1091	1670	232	264	1.14
69/U/900/0	0.80	0.63	0.00	0.63	3.82	325	3.37	1307	835	148	550	76	77	1.01
69/U/900/-8	0.50	0.49	0.00	0.49	3.37	368	3.22	1487	412	42	218	30	34	1.12
Average													1.56	
COV													34%	

413
 414 It is seen that the proposed approach provides a generally conservative method for
 415 the prediction of peak capacity for specimens with reduced cover and a variety of
 416 internal reinforcement arrangements. The coefficient of variation is high, highlighting

417 that whilst conservative, the method should be applied with caution to specimens
 418 outside the boundaries of these data.

419 Specimen 69/U/900/-8 has unenclosed strand and -8mm cover. In this situation the
 420 strand has negligible confinement and any movement perpendicular to the applied load
 421 would cause the strand to 'peel off' from the concrete surface. Such perpendicular
 422 movement was indeed evident in this test, and came about as a direct result of the
 423 specimen rotating slightly, but significantly given the very low embedment depth. The
 424 34kN load achieved in this specimen may be compared to 129kN achieved in
 425 69/E/900/-8, where the test strand is enclosed by transverse reinforcement and, thus,
 426 peeling is prevented.

427 In most structures, prestress losses are not known accurately, and must be
 428 predicted by calculation. Taking a simplified approach of 25% typical losses and setting
 429 $\sigma_{pmoo} = 0.75(\sigma_{pm0})$ reduces the conservativeness of the peak capacity calculations, as
 430 shown in Table 8. Specimens 69/U/900/0 and 69/U/900/-8 now show unconservative
 431 predictions since actual losses were much higher than this simplified approach would
 432 suggest.

433 **Table 8: Peak capacity predictions for all stressed specimens taking $\sigma_{pmoo} = 0.75(\sigma_{pm0})$**

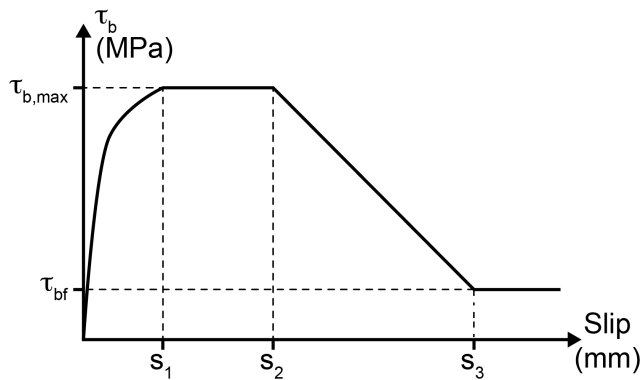
Code	δ_1	δ_2	δ_3	δ_4	$f_{ctm(tr)}$ (MPa)	l_{pl2} (mm)	$f_{ctm(te)}$ (MPa)	l_{bpd} (mm)	$\delta_1 \delta_2 (\sigma_{pl})$ (MPa)	$\delta_1 \delta_2 (\sigma_{pmoo})$ (MPa)	σ_p (MPa)	$F_{reduced}$ (kN)	Experi menta l (kN)	Exp/ Pred
55/E/600/37	1.00	1.00	0.80	1.00	2.25	440	3.50	1117	1670	687	919	128	217	1.70
55/E/600/0	0.80	0.80	0.80	0.63	3.59	276	3.38	976	1069	440	730	102	105	1.03
55/E/600/-8	0.50	0.80	0.80	0.49	2.39	416	2.25	1467	668	275	344	48	84	1.76
69/E/900/37	1.00	1.00	0.80	1.00	2.14	580	2.02	1547	1670	859	1127	157	195	1.24
69/E/900/0	0.80	0.80	0.80	0.63	3.13	397	3.02	1043	1069	550	954	133	131	0.99
69/E/900/-8	0.50	0.80	0.80	0.49	3.64	341	3.67	873	668	344	668	93	129	1.39
55/U/600/37	1.00	1.00	0.00	1.00	3.47	286	2.96	1085	1670	687	1073	149	233	1.56
55/U/600/0	0.80	0.63	0.00	0.63	2.30	431	2.61	1338	835	344	435	60	93	1.54
55/U/600/-8	0.50	0.49	0.00	0.49	3.73	266	3.82	885	412	169	300	42	78	1.87
69/U/900/37	1.00	1.00	0.00	1.00	3.46	358	3.37	938	1670	859	1617	225	264	1.17
69/U/900/0	0.80	0.63	0.00	0.63	3.82	325	3.37	905	835	429	832	116	77	0.67
69/U/900/-8	0.50	0.49	0.00	0.49	3.37	368	3.22	974	412	212	388	54	34	0.63
Average													1.30	
COV													32%	

434
 435 It should be noted that the total prestress losses between tensioning and casting
 436 (Table 4) are particularly high for specimens 69/U/900/0 and 69/U/900/-8 (76% and

437 87% respectively). This degree of prestress loss implies that the strand had slipped
 438 significantly before testing, breaking the bond of the strand to concrete. This explains
 439 the unconservative predictions for these specimens, which are based on the
 440 assumption that some initial bond exists.

441 4.2 Bond-slip modelling

442 No broadly accepted model for the bond-slip behaviour of 7-wire strand is currently
 443 available. The fib Model Code [16] provides an analytical bond stress-slip relationship
 444 for deformed and plain bars that is based on Figure 16 and Eqs.(11)-(14). The bond
 445 stress-slip relationship is influenced by factors which include (i) surface geometry of the
 446 bar; (ii) concrete strength; (iii) casting position; (iv) cover distance; and (v) transverse
 447 confinement, either by reinforcement or applied load.



448

449 **Figure 16: Bond stress-slip model basis [16]**

450
$$\tau_{b0} = \tau_{b,max} \left(s / s_1 \right)^\alpha \quad \text{for } 0 \leq s \leq s_1 \quad (11)$$

451
$$\tau_{b0} = \tau_{b,max} \quad \text{for } s_1 < s \leq s_2 \quad (12)$$

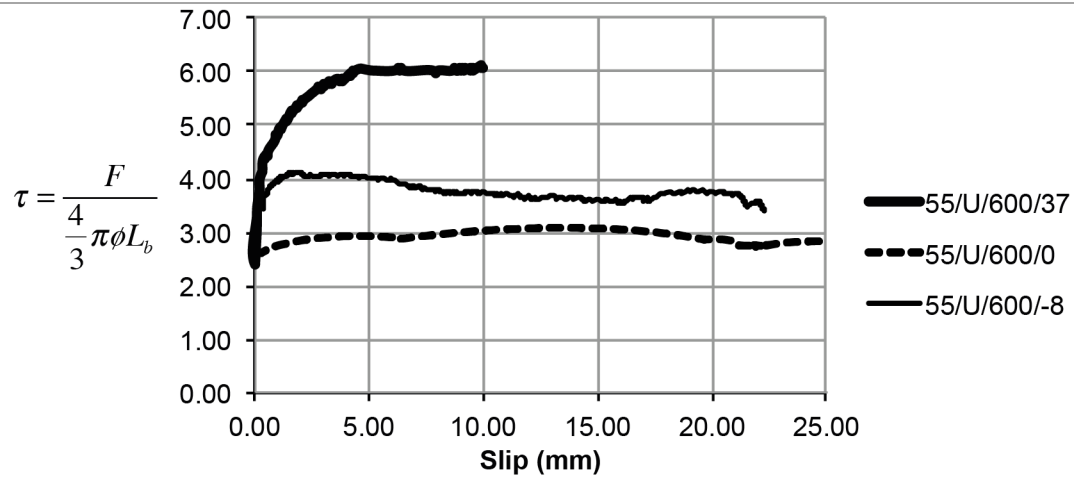
452
$$\tau_{b0} = \tau_{b,max} - (\tau_{b,max} - \tau_{bf}) (s - s_2) / (s_3 - s_2) \quad \text{for } s_2 < s \leq s_3 \quad (13)$$

453
$$\tau_{b0} = \tau_{bf} \quad \text{for } s_3 < s \quad (14)$$

454 The fib Model shown above predicts that deformed bar will achieve a greater peak
455 bond stress (τ_{bmax}) when compared to plain bar, due primarily to the surface geometry
456 of the bar which creates mechanical resistance to slip. In well-confined concrete a
457 plateau at high bond stress can occur during crushing of the concrete between ribs. In
458 unconfined concrete, a large drop in bond stress post-peak would instead be seen in a
459 splitting failure mode.

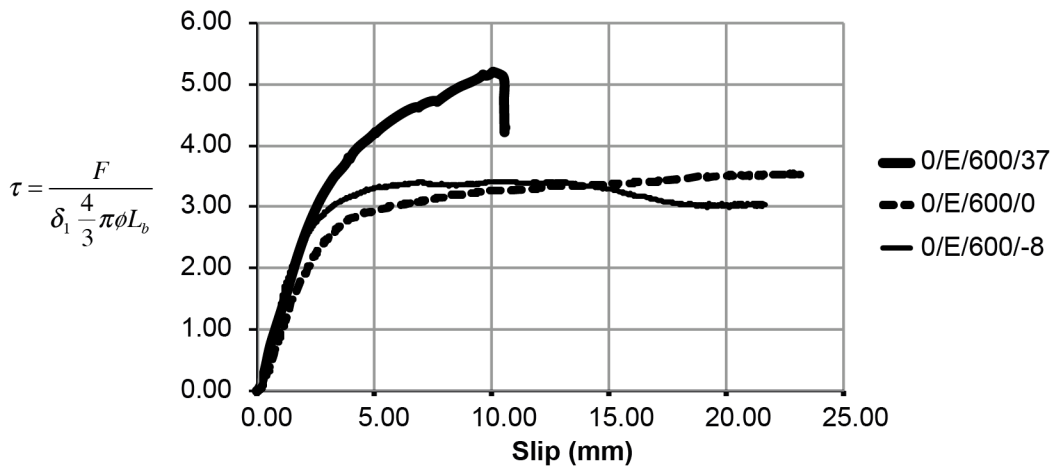
460 For plain bar, once chemical bond is overcome the bar offers little further
461 mechanical resistance to pull out. This is manifested in Figure 16 by setting $\tau_{b,max} = \tau_{bf}$
462 and $s_1 = s_2 = s_3$. The bond stress-slip behaviour of plain bar occurs at much lower
463 stress levels when compared to deformed bar.

464 The test results demonstrate that the bond stress-slip behaviour of strand does not
465 have the characteristic peak of deformed bar (where $\tau_{bmax} > \tau_{bf}$). This is shown for a
466 sample of stressed specimens in Figure 17 and a sample of unstressed specimens in
467 Figure 18. The test data provides only an average bond stress along the bar, as the
468 load in the bar and the slip of the bar could only be measured in one place. This is a
469 clear limitation that neglects the potential for variations in bond along the stressed
470 length of a pull-out test.



471

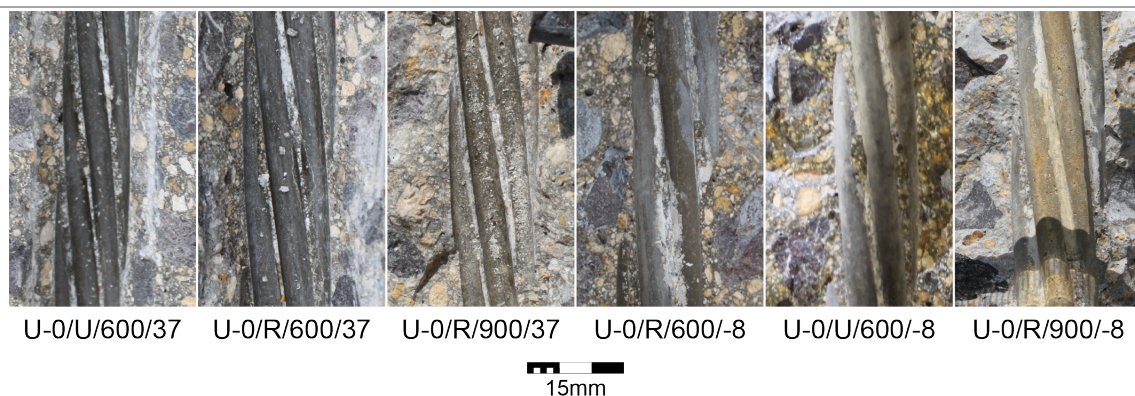
472 **Figure 17: Bond stress-slip (three stressed specimens)**



473

474 **Figure 18: Bond stress-slip (three unstressed specimens)**

475 Inspection of the specimens after testing showed that concrete was not crushed
 476 between the strand wires (Figure 19). Therefore the plain bar model from the fib Model
 477 Code [16] was adapted to produce a strand pull out model as described below.



478

479 **Figure 19: Post-testing examination of concrete surface**

480 **4.2.1 Strand pull out model**

481 The proposed bond stress model is based on the plain bar pull out model of the fib
 482 Model Code [16] method and Eqs.(11)-(14). Proposed parameters for the model are
 483 given in Table 9.

484 **Table 9: Proposed parameters for the strand pull out model**

Parameter	Proposed value – stressed 7-wire strand	Proposed value – unstressed 7-wire strand
$s_1 = s_2 = s_3$ (after FIB [16] and as shown in Figure 16)	0.1mm	2.0mm
α	0.5	0.5
$\tau_{b,max} = \tau_{bf}$	Eq.(15)	Eq.(15)

485
$$\tau_{b,max} = \tau_{bf} = (\delta_1)(\delta_2)(0.70)\sqrt{f_{cm}} \quad (15)$$

486 Where δ_1 accounts for the reduction in bonded perimeter in specimens with reduced
 487 cover (Eq.(2)); δ_2 accounts for confinement from cover or transverse reinforcement
 488 (Eq.(3)); the factor of 0.70 is chosen based on the test results; f_{cm} is the mean concrete
 489 cylinder strength of the specimen.

490 The experimental bond stress is compared to the proposed model in Table 10 for
 491 stressed strand specimens and in Table 11 for the unstressed strand specimens. The
 492 bond stress is calculated using Eq.(16), following the method used by both Mattock (as

493 cited by Tabatabai and Dickson [39]) and Marti-Vargas *et al* [40] to calculate the actual
 494 circumference from nominal strand diameter:

$$495 \quad \tau = \frac{F}{\delta_1 \frac{4}{3} \pi \phi L_b} \quad (16)$$

496 where F is the force in the strand; ϕ is the nominal strand diameter; δ_1 accounts for
 497 reduction in bonded perimeter with reduced cover; and L_b is the bonded length. The
 498 peak bond stress during testing is found by setting $F = F_{max}$, the maximum recorded
 499 force in the strand during testing.

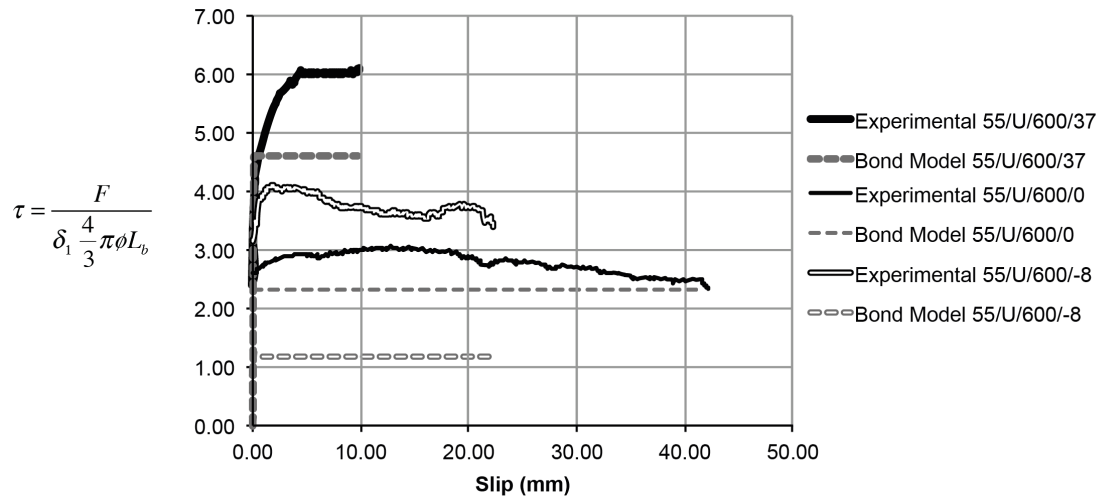
500 **Table 10: Predicted peak bond stress for stressed strand specimens using Eq.(15)**

Code	f_{cm} (MPa) ^a	δ_1	δ_2	δ_3	δ_4	Cover (mm)	Bonded length (mm)	Failure load (kN)	Experimental peak stress (MPa)	Predicted peak stress ^b (MPa)	Experimental / Predicted
55/E/600/37	42.2	1.00	1.00	0.80	1.00	37	600	217	5.68	4.55	1.25
55/E/600/0	42.9	0.80	0.80	0.80	0.63	0	600	105	3.44	2.93	1.17
55/E/600/-8	46.6	0.50	0.80	0.80	0.49	-8	600	84	4.40	1.91	2.30
69/E/900/37	43.8	1.00	1.00	0.80	1.00	37	900	232	4.05	4.63	0.87
69/E/900/0	36.3	0.80	0.80	0.80	0.63	0	900	131	2.86	2.70	1.06
69/E/900/-8	46.8	0.50	0.80	0.80	0.49	-8	900	129	4.50	1.92	2.35
55/U/600/37	43.4	1.00	1.00	0.00	1.00	37	600	233	6.10	4.61	1.32
55/U/600/0	43.7	0.80	0.63	0.00	0.63	0	600	93	3.04	2.31	1.32
55/U/600/-8	47.8	0.50	0.49	0.00	0.49	-8	600	78	4.08	1.19	3.42
69/U/900/37	39.0	1.00	1.00	0.00	1.00	37	900	264	4.61	4.37	1.05
69/U/900/0	47.0	0.80	0.63	0.00	0.63	0	900	77	1.68	2.40	0.70
69/U/900/-8	46.2	0.50	0.49	0.00	0.49	-8	900	34	1.19	1.17	1.01
Average										1.49	
COV										53%	

Notes: ^a mean concrete cylinder strength of the specimen; ^b Eq.(14)

501
 502 The results are illustrated for Specimens 55/U/600/37, 55/U/600/0, and 55/U/600/-8
 503 in Figure 20. The predictions are on average conservative, but the coefficient of
 504 variation is high. Specimens 69/E/900/37 and 69/U/900/0 have mildly unconservative
 505 peak bond stress predictions (average 0.79). The high variation is in part due to the
 506 changing surface area for which the experimental peak stress is calculated. In addition
 507 Eq.(15) does not account for effects in the bonded length of the specimen. In
 508 specimens with 0mm or -8mm cover the strand may be fully debonded over a portion

509 of the intended bond length, meaning that the true bond stress in the bonded portion
 510 would be higher than is predicted by Eq.(15).



511

512 **Figure 20: Comparison of experimental and bond model results for specimens**
 513 **55/U/600/37, 55/U/600/0, and 55/U/600/-8**

514

515 **Table 11: Predicted bond stress for unstressed strand specimens using Eq.(15)**

Code	f_{cm} (MPa) ^(a)	δ_1	δ_2	δ_3	δ_4	Cover (mm)	Bonded length (mm)	Failure load (kN)	Experimental peak stress (MPa)	Predicted peak stress ^(b) (MPa)	Experimental / Predicted
0/P/300/37	42.7	1.00	1.00	0.00	1.00	37	300	85	4.45	4.58	0.97
0/P/300/0	42.7	0.80	0.63	0.00	0.63	0	300	50	3.27	2.29	1.43
0/P/600/37	46.6	1.00	1.00	0.00	1.00	37	600	208	5.44	4.78	1.14
0/P/600/0	46.0	0.80	0.63	0.00	0.63	0	600	79	2.58	2.37	1.09
0/E/300/37	39.8	1.00	1.00	0.80	1.00	37	300	111	5.81	4.42	1.32
0/E/300/0	39.8	0.80	0.80	0.80	0.63	0	300	65	4.25	2.83	1.50
0/E/300/-8	39.3	0.50	0.80	0.80	0.49	-8	300	52	5.44	1.75	3.10
0/E/600/37	42.7	1.00	1.00	0.80	1.00	37	600	199	5.21	4.57	1.14
0/E/600/0	45.8	0.80	0.80	0.80	0.63	0	600	108	3.53	3.03	1.17
0/E/600/-8	43.3	0.50	0.80	0.80	0.49	-8	600	65	3.40	1.84	1.85
0/E/900/37	41.6	1.00	1.00	0.80	1.00	37	900	223	3.89	4.51	0.86
0/E/900/0	42.3	0.80	0.80	0.80	0.63	0	900	159	3.47	2.91	1.19
0/E/900/-8	34.7	0.50	0.80	0.80	0.49	-8	900	124	4.33	1.65	2.62
0/U/600/37	41.7	1.00	1.00	0.00	1.00	37	600	216	5.65	4.52	1.25
0/U/600/0	40.6	0.80	0.63	0.00	0.63	0	600	83	2.72	2.23	1.22
0/U/600/-8	46.3	0.50	0.49	0.00	0.49	-8	600	77	4.03	1.18	3.43
0/U/900/37	48.1	1.00	1.00	0.00	1.00	37	900	250	4.36	4.86	0.90
0/U/900/0	47.3	0.80	0.63	0.00	0.63	0	900	136	2.97	2.41	1.23
0/U/900/-8	46.2	0.50	0.49	0.00	0.49	-8	900	112	3.91	1.17	3.33
Average										1.62	
COV										52%	

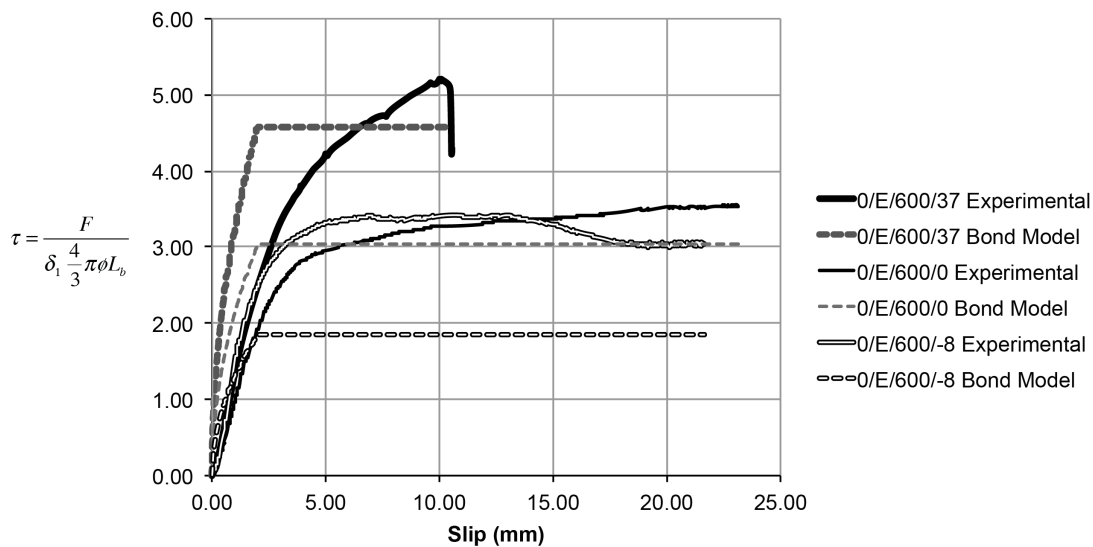
Notes: ^a mean concrete cylinder strength of the specimen; ^b Eq.(14)

516

517 The results are illustrated for Specimens 0/E/600/37, 0/E/600/0, and 0/E/600/-8 in
 518 Figure 21. The predictions shown in Table 11 are on average conservative, but the

519 coefficient of variation is again high. Specimens 0/P/300/37, 0/E/900/37 and
 520 0/U/900/37 have mildly unconservative peak bond stress predictions (average 0.91).

521 The high variability in both data sets could be attributable to the specimens with
 522 partially exposed strand. If specimens with -8mm cover are excluded from the analysis,
 523 the stress predictions are improved slightly. For stressed specimens, the average ratio
 524 is 1.09 with a COV of 20%; for unstressed specimens the ratio is 1.17 with a COV of
 525 16%.



526

527 **Figure 21: Comparison of experimental and bond model results for specimens**
 528 **0/E/600/37, 0/E/600/0, and 0/E/600/-8**

529 **5 Discussion**

530 Accurately determining the behaviour of concrete elements suffering from loss of cover
 531 is of crucial importance when high cost infrastructure is being assessed. A full
 532 understanding of capacity can allow load restrictions and closures to be minimised
 533 prior to appropriate repair work.

534 In this paper it is seen that as cover distances are reduced, ultimate (peak)
 535 capacities and residual capacities also reduce. Specimens with unstressed strand lost

536 up to 67% capacity at -8mm cover when compared to 37mm cover, while specimens
537 with stressed strand lost up to 87% capacity at -8mm cover when compared to 37mm
538 cover.

539 Detailing practice of reinforced concrete members has changed considerably over
540 time, and varies between countries. It is seen that specimens with unenclosed strand,
541 where the transverse reinforcement does not enclose the longitudinal reinforcement,
542 achieved surprisingly high peak capacities. 0/U/600/-8 (unstressed, unenclosed strand
543 with -8mm cover) reached 35% of the capacity of 0/U/600/37 (unstressed, unenclosed
544 strand with 37mm cover).

545 However, it was generally seen that specimens with -8mm and 0mm cover whose
546 strand was enclosed by transverse reinforcement reached a higher peak load than
547 those whose strand was unenclosed, due to the additional confining effect of the
548 transverse reinforcement. In only one case did an unenclosed specimen, 0/U/600/-8,
549 achieved a higher load than the equivalent enclosed specimen, 0/E/600/-8. Specimens
550 with unenclosed strand typically demonstrated post-peak behaviour with a descending
551 load-slip curve.

552 Specimens with less than 0mm cover (i.e. with partially exposed strand)
553 demonstrate highly variable results when attempts are made to predict bond stresses.
554 Small variations in the cover distance, caused by normal construction tolerances, may
555 be critical for this set of tests. A small change in cover distance would potentially lead
556 to a significant percentage change in bonded area and pull out capacity. As shown in
557 §4.2.1, the coefficient of variation of the capacity predictions is improved by excluding
558 negative cover specimens from the analysis. Since only one specimen was tested for
559 each combination of transverse reinforcement arrangement, bond length and cover
560 distance, an accurate measure of this degree of variability is not known.

561 In addition to the pull out testing, the monitoring of strand stress through the casting
562 and detensioning process has provided useful data. Stressed beams with full cover
563 (37mm) saw lower losses between tensioning and testing than those with 0mm and -
564 8mm cover. Specimens 55/U/600/37 and 69/U/900/37, with 37mm cover, both lost 13%
565 of their prestress between tensioning and testing. This compares to losses of up to
566 76% for 69/U/900/0 (0mm cover) and 87% for 69/U/900/-8 (-8mm cover). In both of
567 these situations, the degree of prestress loss has significantly influenced subsequent
568 pull out testing, as the strand can be assumed to have lost significant bond during
569 detensioning prior to testing.

570 The method provides good predictions of peak bond capacity for both stressed and
571 unstressed strand that provides conservative results for all specimens (Table 7).

572 The behaviour of strand during pull out is seen to be similar to plain bar, with a
573 characteristic plateau, but achieves higher bond stresses than would be predicted by a
574 plain bar pull out model. A strand bond stress-slip relationship is proposed, based on
575 the general model given in the fib Model Code [16]. The relationship proposed in
576 Eq.(15) is, on average, conservative for both stressed and unstressed specimen.
577 However, considerable variability in the predictions is again seen (Table 10 and Table
578 11) suggesting that further work is required to identify the controlling parameters for
579 bond modelling.

580 The test results show good correlation between the stressed and unstressed tests
581 undertaken in this investigation, demonstrating that the unstressed method is a suitable
582 proxy for the stressed behaviour. This paper has considered the behaviour of
583 specimens with reduced cover, but does not consider other effects such as corrosion to
584 strands, which may also occur in field conditions.

585 **5.1 Conclusions**

586 The periodic assessment of our existing infrastructure is a crucial part of maintaining
587 appropriate levels of public safety over long periods of time. It is important that realistic
588 predictions of the capacity of existing structures can be made in order to avoid
589 unnecessary and expensive intervention work.

590 This paper has addressed this issue for the case of prestressed concrete beams,
591 which face two main assessment challenges – 1) design and construction practice has
592 changed significantly in the past 50 years, and modern codified approaches can be
593 incompatible with historic designs; and 2) deterioration of exposed soffits can lead to
594 reduced cover to internal prestressing strand.

595 There are currently no widely accepted methods for the prediction of the peak and
596 residual capacity of prestressed concrete beams with inadequately detailed 7-wire
597 strand. This paper presents a new predictive model that has been validated against a
598 new set of experimental results from 31 beam tests, including 19 with unstressed
599 strand and 12 with stressed strand.

600 This paper has investigated in detail for the first time the effect of loss of cover on
601 bond, peak load, and residual load in structures where 7-wire strand is used as flexural
602 reinforcement. The results presented here may be used to support new guidance on
603 appropriate reduction factors for assessment of prestressed concrete elements with
604 inadequately detailed 7-wire strand.

605 **5.2 Future work**

606 In addition to the developments made in this paper, further work is required to fully
607 understand the behaviour of structures deemed to be structurally inadequate. The
608 impact of the in-situ corrosion of strand on bond performance and the effectiveness of

609 repairs to structures with reduced or ineffective cover, are both areas of great
610 importance that need further work.

611 **5.3 Acknowledgements**

612 This work was commissioned by Balfour Beatty Mott MacDonald JV, the Asset Support
613 Contract Provider for Highways England Area 10, as part of a Research project to
614 investigate the actual capacity of half-joints with theoretically inadequate reinforcement
615 detailing. The authors gratefully acknowledge support and advice from Highways
616 England in the preparation of the test program and this paper, and the technician
617 support provided by the University of Bath in constructing and testing the specimens.

618

619

620

References

- 621 [1] ASCE. Infrastructure Report Card. ASCE; 2016.
- 622 [2] HM Treasury. National Infrastructure Plan 2014. London: HM
623 Treasury; 2014.
- 624 [3] Highways Agency. BD57. DESIGN FOR DURABILITY. London:
625 The Stationery Office; 2001.
- 626 [4] Highways Agency. BD 44/15. The Assessment of Concrete Highway
627 Bridges and Structures. London: The Stationery Office; 2015.
- 628 [5] Highways Agency. BA 39/93. ASSESSMENT OF REINFORCED
629 CONCRETE HALF-JOINTS. London: The Stationery Office; 1993.
- 630 [6] The Highways Agency. BD 79/13. THE MANAGEMENT OF SUB-
631 STANDARD HIGHWAY STRUCTURES. London: The Stationery
632 Office; 2013.
- 633 [7] RILEM. RILEM Recommendations for the Testing and Use of
634 Constructions Materials, RC 5 Bond test for reinforcement steel. 1. Beam
635 test. London: E & FN SPON; 1982.
- 636 [8] ASTM. D7913-14. Standard Test Method for Bond Strength of Fiber-
637 Reinforced Polymer Matrix Composite Bars to Concrete by Pullout
638 Testing. West Conshohocken, PA: ASTM International; 2014.
- 639 [9] Haskett M, Oehlers DJ, Ali MS. Local and global bond characteristics
640 of steel reinforcing bars. Engineering Structures. 2008;30:376-83.
- 641 [10] Metelli G, Plizzari G. influence of the relative rib area on bond
642 behaviour. Magazine of Concrete Research. 2014;66:277-94.
- 643 [11] Cairns J, Plizzari G. Towards a harmonised European bond test.
644 Materials and Structures. 2003;36:498-506.
- 645 [12] fib. Bond of reinforcement in concrete. State of art report task group
646 Bond Models. Lausanne: fib; 2000.
- 647 [13] BSI. BS 4449:2005+A3:2016. Steel for the reinforcement of concrete
648 Weldable reinforcing steel Bar, coil and decoiled product Specification.
649 London: BSI; 2016.
- 650 [14] ASTM. A944 - 10. Standard Test Method for Comparing Bond
651 Strength of Steel Reinforcing Bars to Concrete Using Beam-End
652 Specimens. West Conshohocken, PA: ASTM International; 2015.
- 653 [15] Perera K, Ibell T, Darby A. Bond characteristics of near surface
654 mounted CFRP bars. Construction and Building Materials. 2013;43:58-68.

- 655 [16] FIB. Model Code 2010. Volume 1. Lausanne: International
656 Federation of Structural Concrete (fib); 2013.
- 657 [17] Moustafa S. Pull-out strength of strand and lifting loops. Washington:
658 Concrete Technology Corporation; 1974.
- 659 [18] Ramirez JA, Russell BW. Transfer, Development, and Splice Length
660 for Strand/Reinforcement in High-Strength Concrete. NCHRP REPORT
661 603 ed. Washington, DC: Transportation Research Board; 2008.
- 662 [19] ASTM. A1081. Standard Test Method for Evaluating Bond of Seven-
663 Wire Steel Prestressing Strand. West Conshohocken: ASTM International;
664 2012.
- 665 [20] Logan DR. Acceptance Criteria for Bond Quality of Strand for
666 Pretensioned Prestressed Concrete Applications. PCI Journal. 1997;March-
667 April:52-90.
- 668 [21] Rose DR, Russell BW. Investigation of Standardized Tests to Measure
669 the Bond Performance of Prestressing Strand. PCI Journal. 1997;July-
670 August:56-80.
- 671 [22] Briere V, Harries K, Kasan J, Hager C. Dilation behavior of seven-
672 wire prestressing strand – the Hoyer effect. Constr Build Mater.
673 2013;40:650-8.
- 674 [23] Marti-Vargas JR, Serna-Ros P, Fernandez-Prada MA, Miguel-Sosa
675 PF. Test method for determination of the transmission and anchorage
676 lengths in prestressed reinforcement. Magazine of Concrete Research.
677 2006;58:21-9.
- 678 [24] Cousins TE, Badeaux MH, Moustafa S. Proposed test for determining
679 bond characteristics of prestressing strand. PCI Journal. 1992;January-
680 February:66-73.
- 681 [25] Barnes RW, Burns NH. Anchorage Behavior of 15.2 mm (0.6 in)
682 Prestressing Strand in High Strength Concrete. PCI/FHWA/FIB
683 International Symposium on High Performance Concrete. Orlando, FL:
684 PCI; 2000. p. 484–93.
- 685 [26] BSI. BS EN 1992-1-1. Eurocode 2: Design of concrete structures -
686 Part 1-1: General rules and rules for buildings. London, UK: BSI; 2004.
- 687 [27] Tepfers R. A Theory of Bond Applied to Overlapping Tensile
688 Reinforcement Splices for Deformed Bars. Division of Concrete
689 Structures: Chalmers University of Technology, Goteborg, Sweden; 1973.
690 p. 328.

- 691 [28] Galvez JC, Benitez JM, Tork B, Casati MJ, Cendon DA. Splitting
692 failure of precast prestressed concrete during the release of the prestressing
693 force. *Engineering Failure Analysis*. 2009;16:2618-34.
- 694 [29] Den Uijl JA, Bigaj AJ. A bond model for ribbed bars based on
695 concrete confinement. *HERON*. 1996;41:201-26.
- 696 [30] Deatherage JH, Burdette EG. Development length and lateral spacing
697 requirements of prestressing strand for prestressed concrete bridge girders.
698 *PCI Journal*. 1994;January-February:70-83.
- 699 [31] Den Uijl JA. Transfer length of prestressing strand in HPC. *Progress*
700 *in Concrete Research*. 1995;4:75-90.
- 701 [32] Rogers RA, Wotherspoon L, Scott A, Ingham J. Residual strength
702 assessment and destructive testing of decommissioned concrete bridge
703 beams with corroded pretensioned reinforcement. *PCI Journal*.
704 2012;Summer 2012.
- 705 [33] BSI. BS 12390-2. Testing hardened concrete Part 2: Making and
706 curing specimens for strength tests. London: BSI; 2009.
- 707 [34] BSI. BS EN 12390-3. Testing hardened concrete Part 3: Compressive
708 strength of test specimens. London, UK: BSI; 2009.
- 709 [35] BSI. BS EN 12390-6. Testing hardened concrete Part 6: Tensile
710 splitting strength of test specimens. London, UK: BSI; 2009.
- 711 [36] BSI. BS 4449. Steel for the reinforcement of concrete Weldable
712 reinforcing steel Bar, coil and decoiled product Specification. London:
713 BSI; 2005.
- 714 [37] Bridon. High quality prestressing wire & strand for construction
715 product applications. Construction Products. Doncaster: Bridon; ND.
- 716 [38] BSI. prEN 10138-3. Prestressing steels - Part 3: Strand. London: BSI;
717 2000.
- 718 [39] Tabatabai H, Dickson TJ. The History of the Prestressing Strand
719 Development Length Equation. *PCI Journal*. 1993;38.
- 720 [40] Marti-Vargas JR, Serna P, Hale WM. Strand bond performance in
721 prestressed concrete accounting for bond slip. *Engineering Structures*.
722 2013;51:236-44.
- 723